J-PARC-TH-0257

PROCEEDINGS OF SCIENCE

Single static-quark system above T_c investigated by energy-momentum tensor in SU(3) Yang-Mills theory

Masakiyo Kitazawa,[a,b,*] **Ryosuke Yanagihara,**[a] **Masayuki Asakawa**[a] **and Tetsuo Hatsuda**[c]

[a] *Department of Physics, Osaka University, Toyonaka, Osaka 560-0043, Japan*

[b] *J-PARC Branch, KEK Theory Center, Institute of Particle and Nuclear Studies, KEK, 203-1, Shirakata, Tokai, Ibaraki, 319-1106, Japan*

[c] *RIKEN Interdisciplinary Theoretical and Mathematical Sciences Program (iTHEMS), RIKEN, Wako 351-0198, Japan*

E-mail: kitazawa@phys.sci.osaka-u.ac.jp

We investigate the distribution of energy-momentum tensor (EMT) around a static quark in the deconfined phase of SU(3) Yang-Mills theory. The EMT defined through the gradient-flow formalism is used for the numerical analysis of the EMT distribution around the Polyakov loop with the continuum extrapolation. Using EMT, one can study the mechanical distortion of the color gauge field induced by the static charge. We find substantial separation in the absolute values of the EMT eigenvalues which is not observed in Maxwell theory. The separation grows as temperature is lowered toward the critical temperature. The lattice data also indicate the thermal screening at long distance and the perturbative behavior at short distance.

The 38th International Symposium on Lattice Field Theory, LATTICE2021 26th-30th July, 2021 Zoom/Gather@Massachusetts Institute of Technology

*Speaker

PoS(LATTICE2021)396

1. Introduction

One of the fundamental methods to explore a system described by the quantum field theory is to introduce test charge(s) and analyze the response of the system. In this proceedings, we investigate the response of SU(3) Yang-Mills (YM) theory against the existence of a static quark in the deconfined phase in lattice numerical simulations [1]. To study the local distortion of the color field induced by the static charge we use the energy-momentum tensor (EMT), $T_{\mu\nu}(x)$.

Recently, successful analysis of the correlation functions of EMT operators in lattice numerical simulations has become possible thanks to the small-flow time expansion (SFtX) method [2, 3] based on the gradient flow [4–6]. Its application to the analysis of thermodynamics in SU(3) YM theory [7–9] and QCD with fermions [10, 11] shows that this method defines the EMT operator properly and is effective in suppressing statistical errors in numerical simulations. The EMT operator defined in this method has been applied for the analysis of various systems [12–15]. We use this method for the measurement of $T_{\mu\nu}(x)$ in this study.

2. Energy-momentum tensor and stress tensor

The EMT $T_{\mu\nu}(x)$ is related to the stress tensor σ_{ij} as

$$\sigma_{ij} = -T_{ij} \qquad (i,j=1,2,3). \tag{1}$$

The force per unit area $\mathcal{F}_i$ is given by $\mathcal{F}_i = \sigma_{ij}n_j = -T_{ij}n_j$ with the normal vector n_j. The principal axes $n_j^{(k)}$ and the corresponding eigenvalues λ_k of the stress tensor are obtained by the eigenequation

$$T_{ij}n_j^{(k)} = \lambda_k n_i^{(k)} \quad (k=1,2,3), \tag{2}$$

where $\lambda_k < 0$ ($\lambda_k > 0$) means that neighboring volume elements pull (push) each other on the surface with $n_i^{(k)}$.

A system with a single static source has spherical symmetry. We thus employ the spherical coordinate system (r,θ,φ) in the following. The EMT is diagonalized in this coordinate system as

$$T_{\gamma\gamma'}(\boldsymbol{x}) = \mathrm{diag}(T_{44}(r), T_{rr}(r), T_{\theta\theta}(r)) \tag{3}$$

where $\gamma,\gamma' = 4, r, \theta$. Since the azimuthal and polar components degenerate due to the spherical symmetry, $T_{\varphi\varphi}(r) = T_{\theta\theta}(r)$, only independent components are shown in Eq. (3).

In Maxwell theory, EMT is given by the Maxwell stress-energy tensor $T_{\mu\nu}^{\mathrm{Maxwell}} = F_{\mu\rho}F_{\nu\rho} - \frac{1}{4}\delta_{\mu\nu}F_{\rho\sigma}F_{\rho\sigma}$, where $F_{\mu\nu}$ is the field strength. The EMT in a static system is given by

$$T_{\gamma\gamma'}^{\mathrm{Maxwell}}(\boldsymbol{x}) = \frac{1}{2}\mathrm{diag}(-\vec{E}^2(\boldsymbol{x}), -\vec{E}^2(\boldsymbol{x}), \vec{E}^2(\boldsymbol{x})), \tag{4}$$

with $\vec{E}(\boldsymbol{x})$ being the electric field.

3. Gradient flow

In this study we define the local EMT operator $T_{\mu\nu}(x)$ using the small flow-time expansion (SFtX) method [2, 3] based on the gradient flow [4–6]. We consider the pure SU(3) YM gauge theory in Euclidean space defined by the action,

$$S_{\rm YM} = \frac{1}{4g_0^2}\int d^4x\, G^a_{\mu\nu}(x)G^a_{\mu\nu}(x), \tag{5}$$

with the bare gauge coupling g_0 and the field strength $G^a_{\mu\nu}(x)$. The gradient flow in this theory is defined through the evolution equation of the gauge field called the flow equation [5, 6],

$$\frac{dA^a_\mu(t,x)}{dt} = -g_0^2\frac{\delta S_{\rm YM}(t)}{\delta A^a_\mu(t,x)}, \tag{6}$$

with the gauge field $A^a_\mu(x)$ and the initial condition $A^a_\mu(t=0,x) = A^a_\mu(x)$.

Using Eq. (6), the properly renormalized EMT operator is defined with the small t expansion [2]:

$$T_{\mu\nu}(x) = \lim_{t\to 0} T_{\mu\nu}(t,x), \tag{7}$$

$$T_{\mu\nu}(t,x) = c_1(t)U_{\mu\nu}(t,x) + 4c_2(t)\delta_{\mu\nu}\left[E(t,x) - \langle E(t,x)\rangle_0\right], \tag{8}$$

where $\langle E(t,x)\rangle_0$ is the vacuum expectation value. The dimension-four gauge-invariant operators on the right-hand side of Eq. (8) are given by [2]

$$E(t,x) = \frac{1}{4}G^a_{\mu\nu}(t,x)G^a_{\mu\nu}(t,x), \tag{9}$$

$$U_{\mu\nu}(t,x) = G^a_{\mu\rho}(t,x)G^a_{\nu\rho}(t,x) - \delta_{\mu\nu}E(t,x). \tag{10}$$

For the coefficients $c_1(t)$ and $c_2(t)$ in Eq. (8), we use the two-loop perturbative coefficients [9, 16].

4. Lattice setup

A static quark Q on the lattice is represented by the Polyakov loop Ω. The expectation value of $T_{\mu\nu}(x)$ around a static quark Q at the origin is given by

$$\langle T_{\mu\nu}(t,x)\rangle_Q = \frac{\langle T_{\mu\nu}(t,x){\rm Tr}\Omega(\mathbf{0})\rangle}{\langle {\rm Tr}\Omega(\mathbf{0})\rangle} - \langle T_{\mu\nu}(t,x)\rangle, \tag{11}$$

with the Polyakov loop $\Omega(\mathbf{0})$ located at the origin. Note that Eq. (11) is well-defined only when the Z_3 symmetry in SU(3) YM theory is spontaneously broken. When the Z_3 symmetry is not broken, both numerator and denominator of the first term on the right-hand side in Eq. (11) vanish from symmetry. We thus focus on the system in the deconfined phase above the critical temperature T_c in the present study.

Numerical simulations are performed with the Wilson gauge action for four different temperatures, $1.20T_c$, $1.44T_c$, $2.00T_c$, and $2.60T_c$, with the aspect ratio $N_s/N_\tau = 4$ [1]. For each temperature we perform numerical simulations for five lattice spacings to perform the continuum extrapolation. Among them, we exclude the coarsest lattices from the analysis. We employ the

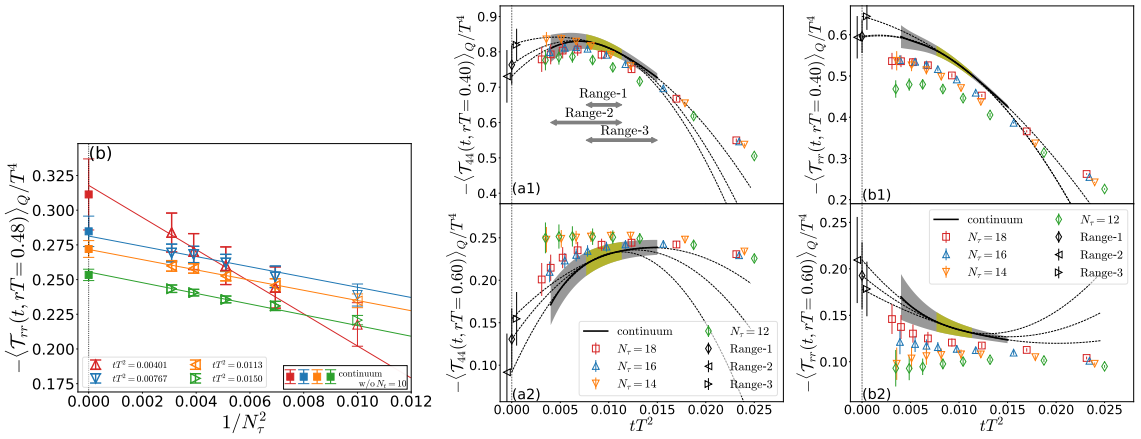

Figure 1: Left: $-\langle T_{rr}(t,rT)\rangle_Q/T^4$ at $T/T_c = 1.44$ and $rT = 0.48$ as functions of $1/N_\tau^2 = a^2T^2$ [1]. The continuum extrapolation is shown by the solid lines and the filled symbols. Middle and right: $-\langle T_{44}(t,rT)\rangle_Q/T^4$ and $-\langle T_{rr}(t,rT)\rangle_Q/T^4$ as functions of tT^2 at $rT = 0.40$ (top) and $rT = 0.60$ (bottom). Open symbols denote $\langle T_{44}(t,rT)\rangle_Q/T^4$ for each a. The black solid line is the continuum-extrapolated result. The dotted lines show the fitted results of the continuum result with Range-1, 2, and 3. The black symbols at $tT^2 = 0$ are the results of the $t \to 0$ extrapolation.

Wilson gauge action for the flow action $S_{\rm YM}(t)$ in Eq. (6) and the clover-type representation for the field strength $G_{\mu\nu}(t,x)$. In the measurement of the Polyakov loop, we apply the multi-hit procedure to suppress the statistical noise [1].

The renormalized EMT distribution around Q is obtained after taking the double extrapolation,

$$\langle T_{\mu\nu}(x)\rangle_Q = \lim_{t\to 0}\lim_{a\to 0}\langle T_{\mu\nu}(t,x)\rangle_Q. \tag{12}$$

In our numerical analysis, we extract the EMT distribution by fitting the lattice data obtained at the lattice spacing a with the following functional form [8, 12]:

$$\langle T_{\mu\nu}(t,x)\rangle_Q = \langle T_{\mu\nu}(x)\rangle_Q + b_{\mu\nu}(t)a^2 + c_{\mu\nu}t + d_{\mu\nu}t^2, \tag{13}$$

where the contributions from discretization effects ($b_{\mu\nu}$) as well as the dimension-six and -eight operators ($c_{\mu\nu}$ and $d_{\mu\nu}$) are considered.

To carry out the double extrapolation Eq. (13), we first take the continuum limit with fixed t, and then carry out the $t \to 0$ extrapolation. In the left panel of Fig. 1, we show $-\langle T_{rr}(t,rT)\rangle_Q$ at $rT = 0.48$ as a function of $1/N_\tau^2 = (aT)^2$ for four values of tT^2. In the panel, the fitting results of the continuum extrapolation according to Eq. (13) at fixed t are shown by the solid lines together with the results of the continuum limit on the vertical dotted line at $1/N_\tau^2 = 0$.

In the middle and right panels of Fig. 1, we show the values of $\langle T_{44}(t,rT)\rangle_Q$ and $\langle T_{rr}(t,rT)\rangle_Q$ at $rT = 0.40$ and 0.60 for each lattice spacing. The results of the continuum limit are denoted by the black solid lines with the gray statistical error band. Using the continuum-extrapolated result, we take $t \to 0$ extrapolation with Eq. (13) at $a = 0$. For the fitting, we employ three fitting ranges of t, Range-1, 2, 3, shown in the middle panel, which are chosen within the range of t that avoids over-smearing due to the gradient flow and at the same time the discretization effects are well suppressed.

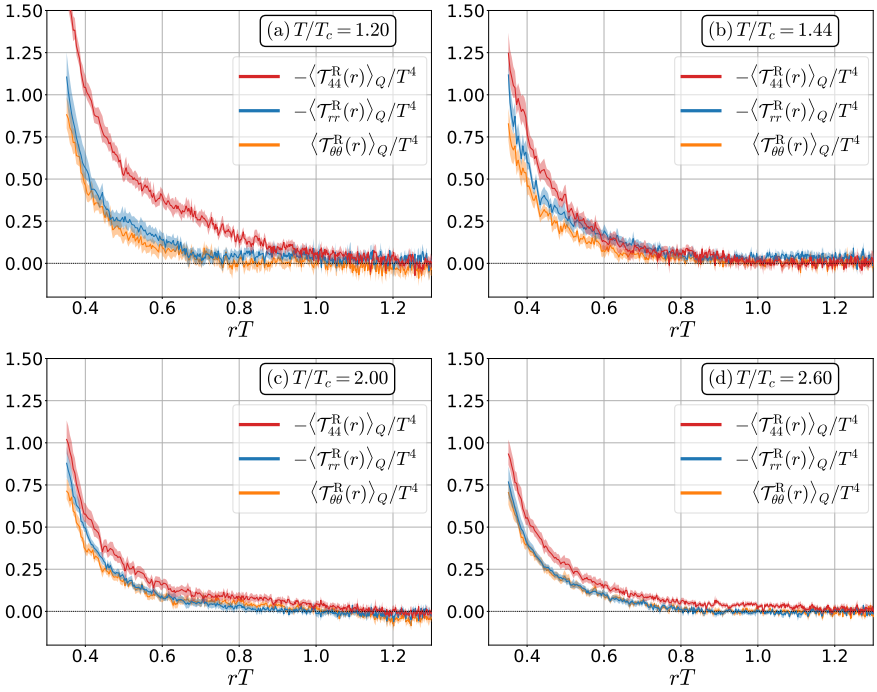

Figure 2: EMT distribution $(-\langle T_{44}(r)\rangle_Q, -\langle T_{rr}(r)\rangle_Q, \langle T_{\theta\theta}(r)\rangle_Q)$ as functions of rT after the double extrapolation [1].

5. Numerical results

In Fig. 2, we show the dimensionless EMT, $-\langle T_{44}(r)\rangle_Q/T^4$, $-\langle T_{rr}(r)\rangle_Q/T^4$, and $\langle T_{\theta\theta}(r)\rangle_Q/T^4$, as functions of rT. The error bands include both the statistical and systematic errors. We find that $-\langle T_{44}(r)\rangle_Q$, $-\langle T_{rr}(r)\rangle_Q$, and $\langle T_{\theta\theta}(r)\rangle_Q$ are all positive for $rT \lesssim 1$ and decrease rapidly with increasing r. These signs are the same as those of the EMT in the Maxwell theory Eq. (4). The positive sign of $-\langle T_{44}(r)\rangle_Q$ means that the energy density is positive, while the signs of $-\langle T_{rr}(r)\rangle_Q$ and $\langle T_{\theta\theta}(r)\rangle_Q$ show that the volume element receives pulling and pushing forces along the longitudinal and transverse directions, respectively. Figure 2 indicates that the absolute values of the spatial components $|\langle T_{rr}(r)\rangle_Q|$ and $|\langle T_{\theta\theta}(r)\rangle_Q|$ are degenerated within the error for all temperatures. On the other hand, $|\langle T_{44}(r)\rangle_Q|$ is larger than the spatial components especially at lower temperature. This is in contrast to the degenerate magnitude of all components in the Maxwell stress Eq. (4). It is interesting to note that such a separation is also obtained in the thermal perturbation theory [17].

In Fig. 3, we show the distribution of EMT in a different normalization. Now we show $r^4\langle T_{\gamma\gamma}(r)\rangle_Q$ as a function of r [fm] in physical units. The distribution of the trace of EMT

$$\Delta_Q(r) \equiv -\langle T_{\mu\mu}(r)\rangle_Q = -\langle T_{44}(r) + T_{rr}(r) + 2T_{\theta\theta}(r)\rangle_Q. \tag{14}$$

is also shown in the figure. From the figure one finds that the EMT distributions have small T dependence at short distances, while sizable T dependence emerges for large distances. This result is reasonable since the T dependence of $r^4\langle T_{\gamma\gamma'}(r)\rangle_Q$ would be suppressed for $r \lesssim (2\pi T)^{-1}$.

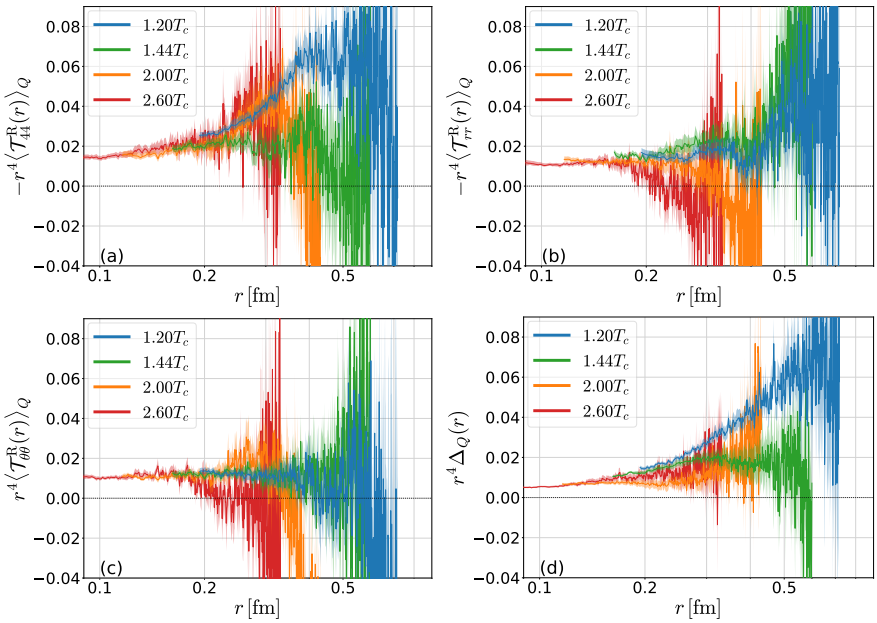

Figure 3: EMT distribution $r^4(-\langle T_{44}(r)\rangle_Q, -\langle T_{rr}(r)\rangle_Q, \langle T_{\theta\theta}(r)\rangle_Q)$ and $r^4\Delta_Q(r)$ as functions of r [fm] for four temperatures [1].

In the leading order perturbation theory in this regime, we have the following ratio

$$\left|\frac{\Delta_Q(r)}{\langle T_{44,rr,\theta\theta}(r)\rangle_Q}\right| = \frac{11}{2\pi}\alpha_s + O(g^3), \tag{15}$$

which is independent of r and T and is given only by a function of α_s. The value of α_s estimated from Eq. (15) is $\alpha_s = 0.22 - 0.32$ depending on the channel at $r = 0.1$ fm [1].

At the long-distance region in Fig. 3, owing to the large errors in this region it is difficult to extract the thermal screening of the form $\exp(-2m_{\rm D}r)$ with the Debye screening mass $m_{\rm D}$. Nevertheless, Fig. 3 shows that the EMT distribution decreases faster than $1/r^4$ in this region, and the tendency becomes more prominent at higher temperatures. To draw a definite conclusion, however, higher statistical data are necessary.

6. Summary and Concluding remarks

In this proceedings we have studied the EMT distribution around a static quark in the SU(3) YM theory at finite temperature above T_c [1]. We have used the SFtX method based on the gradient flow to define the EMT operator on the lattice. We found a substantial difference between the EMT distribution in the temporal direction and that of the spatial directions, especially near T_c. This separation is a unique feature of the YM theory that is not observed in the Maxwell theory.

There are interesting future problems. First, the extension of the present study to full QCD is an important next step. Although the present analysis in the SU(3) YM theory was restricted to $T > T_c$, because the Z_3 symmetry is explicitly broken by dynamical fermions, the present method can be applied directly to a single static quark Q, as well as static QQ and $Q\bar{Q}$ systems, both at low and high temperatures. In particular, the single quark system in QCD at zero temperature corresponds

to a heavy-light meson. The analysis of this system thus provides us with the gravitational form factor of the heavy-light meson at zero and non-zero temperatures.

The numerical simulation of this study was carried out on OCTOPUS at the Cybermedia Center, Osaka University and Reedbush-U at Information Technology Center, The University of Tokyo. This work was supported by JSPS Grant-in-Aid for Scientific Researches, 18H03712, 18H05236, 18K03646, 19H05598, 20H01903.

References

[1] R. Yanagihara, M. Kitazawa, M. Asakawa and T. Hatsuda, *Distribution of Energy-Momentum Tensor around a Static Quark in the Deconfined Phase of SU(3) Yang-Mills Theory*, Phys. Rev. D **102** (2020) 114522 [arXiv:2010.13465 [hep-lat]].

[2] H. Suzuki, *Energy–momentum tensor from the Yang–Mills gradient flow*, PTEP **2013** (2013) 083B03 [arXiv:1304.0533 [hep-lat]].

[3] H. Makino and H. Suzuki, *Lattice energy–momentum tensor from the Yang–Mills gradient flow—inclusion of fermion fields*, PTEP **2014** (2014) 063B02 [arXiv:1403.4772 [hep-lat]].

[4] R. Narayanan and H. Neuberger, *Infinite N phase transitions in continuum Wilson loop operators*, JHEP **03** (2006) 064 [arXiv:hep-th/0601210 [hep-th]].

[5] M. Lüscher, *Properties and uses of the Wilson flow in lattice QCD*, JHEP **08** (2010) 071 [arXiv:1006.4518 [hep-lat]].

[6] M. Luscher and P. Weisz, *Perturbative analysis of the gradient flow in non-abelian gauge theories*, JHEP **02** (2011) 051 [arXiv:1101.0963 [hep-th]].

[7] M. Asakawa *et al.*, *Thermodynamics of SU(3) gauge theory from gradient flow on the lattice*, Phys. Rev. D **90** (2014) 011501 [arXiv:1312.7492 [hep-lat]];

[8] M. Kitazawa, T. Iritani, M. Asakawa, T. Hatsuda, and H. Suzuki, *Equation of State for SU(3) Gauge Theory via the Energy-Momentum Tensor under Gradient Flow*, Phys. Rev. D **94** (2016) 114512 [arXiv:1610.07810 [hep-lat]].

[9] T. Iritani, M. Kitazawa, H. Suzuki, and H. Takaura, *Thermodynamics in quenched QCD: energy–momentum tensor with two-loop order coefficients in the gradient-flow formalism*, PTEP **2019** (2019) 023B02 [arXiv:1812.06444 [hep-lat]].

[10] Y. Taniguchi, et al., *Exploring $N_f = 2+1$ QCD thermodynamics from the gradient flow*, Phys. Rev. D **96** (2017) no.1, 014509 [arXiv:1609.01417 [hep-lat]].

[11] Y. Taniguchi, et al., *$N_f = 2+1$ QCD thermodynamics with gradient flow using two-loop matching coefficients*, Phys. Rev. D **102** (2020) 014510 [arXiv:2005.00251 [hep-lat]].

[12] M. Kitazawa, T. Iritani, M. Asakawa and T. Hatsuda, *Correlations of the energy-momentum tensor via gradient flow in SU(3) Yang-Mills theory at finite temperature*, Phys. Rev. D **96** (2017) 111502 [arXiv:1708.01415 [hep-lat]].

[13] R. Yanagihara, T. Iritani, M. Kitazawa, M. Asakawa and T. Hatsuda, *Distribution of Stress Tensor around Static Quark–Anti-Quark from Yang-Mills Gradient Flow*, Phys. Lett. B **789** (2019) 210 [arXiv:1803.05656 [hep-lat]].

[14] M. Kitazawa, S. Mogliacci, I. Kolbé and W. A. Horowitz, *Anisotropic pressure induced by finite-size effects in SU(3) Yang-Mills theory*. Phys. Rev. D **99** (2019) 094507 [arXiv:1904.00241 [hep-lat]].

[15] R. Yanagihara and M. Kitazawa, *A study of stress-tensor distribution around the flux tube in the Abelian–Higgs model*. PTEP **2019** (2019) 093B02 [arXiv:1905.10056 [hep-ph]].

[16] R. V. Harlander, Y. Kluth and F. Lange, *The two-loop energy–momentum tensor within the gradient-flow formalism*, Eur. Phys. J. C **78** (2018) 944 [arXiv:1808.09837 [hep-lat]].

[17] M. Berwein, private communication.